Journal of Hydrology 252 (2001) 37–50

Journal of Hydrology

www.elsevier.com/locate/jhydrol

On the horizontal-well pumping tests in anisotropic confined aquifers

Hongbin Zhan[a,*], Lihong V. Wang[b,1], Eungyu Park[a]

[a]Department of Geology and Geophysics, Texas A & M University, College Station, TX 77843-3115, USA

[b]Biomedical Engineering Program, Texas A & M University, College Station, TX 77843-3120, USA

Received 20 September 2000; revised 26 March 2001; accepted 14 May 2001

Abstract

A method that directly solves the boundary problem of flow to a horizontal-well in an anisotropic confined aquifer is provided. This method solves the point source problem first, and then integrates the point source solution along the horizontal well axis to obtain the horizontal well solution. The short and long time approximations of drawdowns are discussed and are utilized in the semilog analysis of the drawdown. A closed-form analytical solution of geometrical skin effect at the wellbore is derived. Type curves and derivative type curves of horizontal pumping wells are generated using the CHOW program. This program also calculates the drawdown at any given observation well at any given time. The horizontal-well type curves are different from the vertical-well type curves at early time, reflecting the different nature of flow to a horizontal-well and to a vertical-well. The horizontal-well type curves converge to the vertical-well type curves at late time, showing the similar nature of flow to a horizontal-well and to a vertical-well at late time. The sensitivity of the type curves and derivative type curves on monitoring well location, aquifer anisotropy, horizontal well depth, and horizontal well length is tested. These type curves and derivative type curves can be used in the matching point method for interpreting the pumping test data.

Keywords: Horizontal-well; Pumping-test; Type-curve; Derivative

1. Introduction

Horizontal-wells have been broadly used in the petroleum industry in the past fifteen years. Pressure behavior of horizontal-well pumping in petroleum reservoirs has been studied, with interpretations of pressure data often proving challenging (Goode and Thambynayagam, 1987; Daviau et al., 1988; Ozkan et al., 1989; Rosa and Carvalho, 1989). The difficulty in interpretation is caused by a combined impact upon the pressure distribution from confining boundaries and a finite well screen length.

Horizontal-wells have advantages in at least two scenarios of environmental and hydrological applications. The first is a situation in which direct site access is forbidden or difficult, exemplified by permanent surface constructions, ponds, wetlands, or landfills above the site area. Another scenario is a dense-non-aqueous-phase-liquids (DNAPLs) contaminated site in which DNAPLs sink to the aquifer bottom. Shallow horizontal-wells are also commonly used in air sparging and vent extractions. Advantages in some situations, combined with reduced operational cost have led to increasing utilization of horizontal-well

* Corresponding author. Tel.: +1-979-862-7961; fax: +1-979-845-6162.

E-mail addresses: zhan@hydrog.tamu.edu (H. Zhan), lwang@tamu.edu (L.V. Wang).

[1] Tel.: +1-979-847-9040, Fax: +1-979-845-4450.

0022-1694/01/$ - see front matter
PII: S0022-1694(01)00453-X

Nomenclature

d	aquifer thickness (m)
K_0	the modified Bessel function of second kind and order zero
K_h	horizontal hydraulic conductivity (m/s)
K_z	vertical hydraulic conductivity (m/s)
L	horizontal-well screen length (m)
L_D	dimensionless horizontal-well screen length defined as $L_D = L/d\sqrt{K_z/K_h}$
Q	horizontal-well pumping rate (m^3/s)
r_D	dimensionless horizontal distance from an observation well to a horizontal-well (m), $r_D = [x_D^2 + y_D^2]^{1/2}$
r_w	radius of a horizontal-well (m)
r_{wD}	dimensionless radius of a horizontal-well
s	drawdown (m)
s_D	dimensionless drawdown defined in Eq. (6)
s'_D	dimensionless drawdown in the Laplace domain
s_{HD}	dimensionless drawdown of the horizontal-well
s'_{HD}	dimensionless drawdown of the horizontal-well in the Laplace domain
S_s	specific storativity (m^{-1})
t	time (s)
t_0	time when drawdown equals zero (s)
t_D	dimensionless time defined in Eq. (6)
x	off-center coordinate along the well axis (m)
x_D	dimensionless x defined in Eq. (6)
y	horizontal coordinate perpendicular to the well axis (m)
y_D	dimensionless horizontal coordinate perpendicular to the well axis
z	vertical coordinate (m)
z_D	dimensionless vertical coordinate
z_w	distance from the horizontal-well to the bottom boundary (m)
z_{wD}	dimensionless z_w defined in Eq. (6)
x_0, y_0, z_0	coordinates of the point source (m)
x_{0D}, y_{0D}, z_{0D}	dimensionless coordinates of the point source
α	geometrical skin effect defined in Eq. (31)

technology in hydrological applications in recent years (Langseth, 1990; Tarshish, 1992; Cleveland, 1994; Sawyer and Lieuallen-Dulam, 1998; Zhan, 1999; Zhan and Cao, 2000).

Hantush and Papadopulos (1962) have performed an early investigation on fluid flow into a collector well, which includes a series of jointed horizontal-wells. They provided an analytical solution of the long time approximation of drawdown distribution around collector wells. No detail of derivation was provided in their paper and no solutions were given for the short and intermediate times. Tarshish (1992) constructed a mathematical model of flow in an aquifer with a horizontal-well located beneath a water reservoir. Falta (1995) has developed analytical solutions of transient and steady-state gas pressure and steady-state stream functions resulting from gas injection and extraction from a pair of parallel horizontal-wells. Rushing (1997) has established a semianalytical model for horizontal-well slug testing in confined aquifers. Zhan (1999) and Zhan and Cao (2000) have investigated capture times of horizontal-wells, where the capture time is defined as the time a fluid particle takes to flow to the well. Murdoch (1994) has studied ground water flow to an interceptor trench, and Hunt and Massmann (2000) have recently

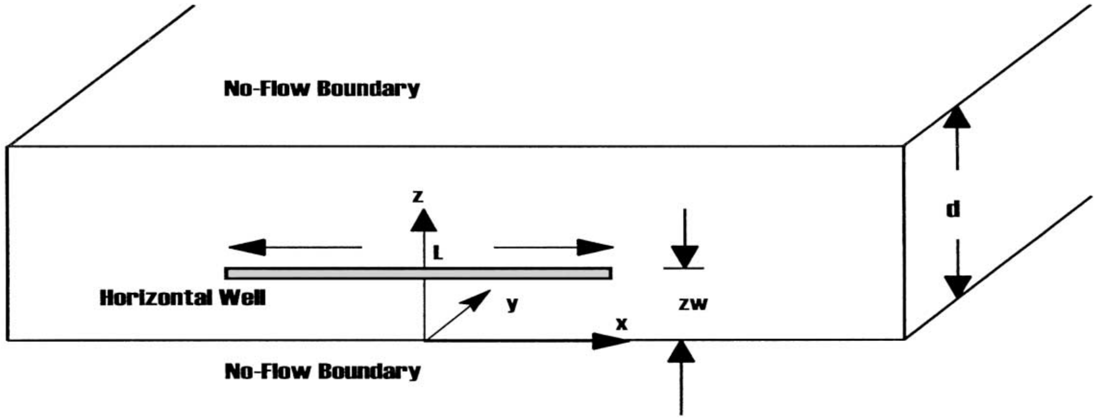

Fig. 1. Schematic diagram of a horizontal-well in a confined aquifer.

investigated vapor flow to a trench. Cleveland (1994) and Sawyer and Lieuallen-Dulam (1998) have compared the recovery efficiency of horizontal and vertical wells. Petroleum engineers have studied the pressure changes in oil reservoirs due to horizontal pumping wells (Goode and Thambynayagam, 1987; Daviau et al., 1988; Ozkan et al., 1989; Rosa and Carvalho, 1989). Many of those works in petroleum engineering use the source function and Green's function methods proposed by Gringarten and Ramey (1973) and Gringarten et al. (1974).

In this paper, a method is proposed to directly solve the boundary problem of ground water flow to a horizontal-well, and solutions of drawdowns are provided. A closed-form solution of wellbore geometrical skin effect is derived. Computer software based on the analytical study of this paper is written. This software can calculate the drawdown of a horizontal pumping well at any given time for either one of the following three monitoring schemes: a fully and a partially penetrating vertical observation wells, and an observation piezometer (a point). The software also provides type curves and derivative type curves for horizontal pumping wells. Applications of the analytical solutions and computer software for horizontal-well pumping tests are discussed last.

2. Ground water flow to a horizontal-well in an anisotropic confined aquifer

Fig. 1 is a schematic diagram of the coordinate system setup and a horizontal-well in a confined aquifer. The x- and y-axes are in the horizontal directions and the z-axis is in the vertical direction. The origin is at the bottom of the aquifer. The well is along the x-axis and its center is at $(0, 0, z_w)$, where z_w is the distance from the well to the bottom boundary. The lateral boundaries are sufficiently distant so as not to influence the flow. The top and bottom boundaries are impermeable. We assume that the hydraulic conductivities in the x and y directions are the same, but they are different from the hydraulic conductivity in the vertical direction.

2.1. Ground water flow to a point source in an anisotropic confined aquifer

Before solving the problem of groundwater flow to a horizontal-well, we first solve the problem of ground water flow to a point source. The governing equation and the associated initial and boundary conditions for a point source pumping in an anisotropic aquifer are:

$$S_s \frac{\partial h}{\partial t} = K_h \frac{\partial^2 h}{\partial x^2} + K_h \frac{\partial^2 h}{\partial y^2} + K_z \frac{\partial^2 h}{\partial z^2} - Q\delta(x - x_0)\delta(y - y_0)\delta(z - z_0) \quad (1)$$

$$h(x, y, z, t = 0) = h_0 \quad (2)$$

$$\partial h(x, y, z = 0, t)/\partial z = 0 \quad (3)$$

$$\partial h(x, y, z = d, t)/\partial z = 0 \quad (4)$$

$$h(x = \pm\infty, y, z, t) = h(x, y = \pm\infty, z, t) = h_0 \quad (5)$$

where S_s is the specific storativity (m^{-1}); h, the hydraulic head (m); t, the time (s); K_h, K_z, the hydraulic conductivities (m/s) in the horizontal and vertical directions, respectively; Q, the pumping rate (m^3/s) ($Q > 0$ for pumping and $Q < 0$ for injecting); δ, the Dirac delta function (m^{-1}); h_0, the initial hydraulic head (m); d, the aquifer thickness (m); and (x_0, y_0, z_0) is the source location. The point source is included as a Dirac delta function in Eq. (1).

We change the hydraulic head h to drawdown $s = h_0 - h$ and define the following dimensionless parameters:

$$s_D = \frac{2\pi K_h d}{Q} s,\ \ t_D = \frac{K_z}{S_s d^2} t,\ \ x_D = \frac{x}{d}\sqrt{\frac{K_z}{K_h}},\ \ y_D = \frac{y}{d}\sqrt{\frac{K_z}{K_h}},\ \ z_D = \frac{z}{d} \tag{6}$$

where s_D, t_D, x_D, y_D, and z_D are the dimensionless counterparts of s, t, x, y, and z, respectively. The dimensionless flow equation and initial and boundary conditions become:

$$\frac{\partial s_D}{\partial t_D} = \frac{\partial^2 s_D}{\partial x_D^2} + \frac{\partial^2 s_D}{\partial y_D^2} + \frac{\partial^2 s_D}{\partial z_D^2} + 2\pi\delta(x_D - x_{0D})\delta(y_D - y_{0D})\delta(z_D - z_{0D}) \tag{7}$$

$$s_D(x_D, y_D, z_D, 0) = 0 \tag{8}$$

$$\partial s_D(x_D, y_D, 0, t_D)/\partial z_D = 0 \tag{9}$$

$$\partial s_D(x_D, y_D, 1, t_D)/\partial z_D = 0 \tag{10}$$

$$s_D(\pm\infty, y_D, z_D, t_D) = s_D(x_D, \pm\infty, z_D, t_D) = 0 \tag{11}$$

where x_{0D}, y_{0D}, and z_{0D} are the dimensionless counterparts of x_0, y_0, and z_0, respectively.

Conducting the Laplace transform to Eq. (7) and boundary conditions (9)–(11) results in

$$ps'_D = \frac{\partial^2 s'_D}{\partial x_D^2} + \frac{\partial^2 s'_D}{\partial y_D^2} + \frac{\partial^2 s'_D}{\partial z_D^2} + \frac{2\pi\delta(x_D - x_{0D})\delta(y_D - y_{0D})\delta(z_D - z_{0D})}{p} \tag{12}$$

$$\partial s'_D(x_D, y_D, 0, p)/\partial z_D = 0 \tag{13}$$

$$\partial s'_D(x_D, y_D, 1, p)/\partial z_D = 0 \tag{14}$$

$$s'_D(\pm\infty, x_D, z_D, p) = s'_D(x_D, \pm\infty, z_D, p) = 0 \tag{15}$$

where p is the Laplace parameter referred to the dimensionless time,s'_D is the dimensionless drawdown in the Laplace domain. Eq. (12) is solved in the Appendix and the result is

$$s'_D(p) = \frac{1}{p} K_0(r_D\sqrt{p}) + \frac{2}{p}\sum_{n=1}^{\infty} \cos(n\pi z_D)\cos(n\pi z_{wD}) \times K_0\left(r_D\sqrt{n^2\pi^2 + p}\right) \tag{16}$$

where $r_D = [(x_D - x_{0D})^2 + (y_D - y_{0D})^2]^{1/2}$, and $z_{wD} = z_w/d$.

Using the inverse Laplace transform table of Hantush (1964, p. 303), the dimensionless drawdown of a point source in real time is obtained analytically as

$$s_D(t_D) = \frac{1}{2} W\left[\frac{r_D^2}{4t_D}\right] + \sum_{n=1}^{\infty} \cos(n\pi z_D)\cos(n\pi z_{wD}) \times W\left[\frac{r_D^2(x'_D)}{4t_D}, n\pi r_D\right] \tag{17}$$

where $W[u]$ and $W[u, v]$ are the well function and leaky well function, respectively (Hantush, 1964).

2.2. Ground water flow to a horizontal-well in an anisotropic confined aquifer

It is generally agreed that the use of a uniform-head boundary to simulate a horizontal-well is closer to physical reality, but this boundary is difficult to incorporate in analytical studies (Rosa and Carvalho, 1989). Instead, a uniform-flux boundary is easier to implement and commonly used (Daviau et al., 1988; Langseth, 1990; Cleveland, 1994).

We test a hypothetical case of a 40 m long horizontal-well in a 20 m thick confined aquifer under both uniform-flux and uniform-head wellbore conditions using VISUAL MODFLOW software (Waterloo Hydrogeologic, 2000). The uniform-head wellbore is simulated by assigning an extremely large hydraulic conductivity, to each of the cells representing the horizontal-well. The numerical simulations show that when the distance between a measured point to a well end is ten times that of the horizontal-well diameter, the discrepancy of the uniform-flux and the uniform-head results is less than 5%. If using a 0.15 m diameter horizontal-well, this implies that when the monitoring well is 1.52 m away from the well end, there is less than 5% difference between the uniform-flux and the uniform-head solutions. This finding agrees with a previous study of Rosa and Carvalho (1989), who had performed an analysis on the geometrical skin effect difference between a uniform-flux and a uniform-head boundaries. In one example shown in Fig. 4 of Rosa and Carvalho (1989), they found that the geometrical skin effect were about 0.9075 and 0.8717 for a uniform-flux and a uniform-head solution, respectively. The difference of these two geometrical skin effects was less than 5%.

Thus, one can employ an approximation of uniform strength of sinks for practical hydrogeological applications. Such a treatment is consistent with previous studies (Hantush and Papadopulos, 1962; Daviau et al., 1988; Ozkan et al., 1989; Rosa and Carvalho, 1989). If treating a horizontal-well as a uniform-flux source along the x direction in the xz plane (see Fig. 1), the drawdown of the horizontal pumping well is obtained through an integration of the point source solution along the well axis. In the Laplace domain, the result is

$$s'_{\mathrm{HD}}(p) = \frac{1}{L_{\mathrm{D}}}\left[\int_{-L_{\mathrm{D}}/2}^{L_{\mathrm{D}}/2} \frac{1}{p} K_0[\sqrt{p}\, r_{\mathrm{D}}(x'_{\mathrm{D}})]\mathrm{d}x'_{\mathrm{D}} + 2\sum_{n=1}^{\infty} \cos[n\pi z_{\mathrm{D}}]\cos[n\pi z_{\mathrm{wD}}] \times \int_{-L_{\mathrm{D}}/2}^{L_{\mathrm{D}}/2} \frac{1}{p} K_0[\sqrt{n^2\pi^2 + p}\, r_{\mathrm{D}}(x'_{\mathrm{D}})]\mathrm{d}x'_{\mathrm{D}}\right] \tag{18}$$

In the real time domain, the result is

$$s_{\mathrm{HD}}(t_{\mathrm{D}}) = \frac{1}{2L_{\mathrm{D}}}\left[\int_{-L_{\mathrm{D}}/2}^{L_{\mathrm{D}}/2} W\left[\frac{r_{\mathrm{D}}^2(x'_{\mathrm{D}})}{4t_{\mathrm{D}}}\right]\mathrm{d}x'_{\mathrm{D}} + 2\sum_{n=1}^{\infty} \cos[n\pi z_{\mathrm{D}}]\cos[n\pi z_{\mathrm{wD}}] \int_{-L_{\mathrm{D}}/2}^{L_{\mathrm{D}}/2} \times W\left[\frac{r_{\mathrm{D}}^2(x'_{\mathrm{D}})}{4t_{\mathrm{D}}}, n\pi r_{\mathrm{D}}(x'_{\mathrm{D}})\right]\mathrm{d}x'_{\mathrm{D}}\right] \tag{19}$$

where $s'_{\mathrm{HD}}(p)$ and $s_{\mathrm{HD}}(t_{\mathrm{D}})$ are the dimensionless drawdowns in the Laplace domain and the real time domain for a horizontal-well, respectively. L_{D} is the dimensionless well screen length defined as $L_{\mathrm{D}} = L/d\sqrt{K_z/K_{\mathrm{h}}}$, $r_{\mathrm{D}}(x'_{\mathrm{D}})$ is

$$r_{\mathrm{D}}(x'_{\mathrm{D}}) = [(x_{\mathrm{D}} - x'_{\mathrm{D}})^2 + y_{\mathrm{D}}^2]^{1/2} \tag{20}$$

We also can express Eq. (19) in an alternative format with an integration to time. Notice that the well functions can be written in the following formats if assigning $u = r_{\mathrm{D}}^2(x'_{\mathrm{D}})/4\tau$:

$$W\left[\frac{r_{\mathrm{D}}^2(x'_{\mathrm{D}})}{4t_{\mathrm{D}}}\right] = \int_{r_{\mathrm{D}}^2(x'_{\mathrm{D}})/4t_{\mathrm{D}}}^{\infty} \frac{1}{u}\mathrm{e}^{-u}\mathrm{d}u = \int_0^{t_{\mathrm{D}}} \frac{1}{\tau}\exp\left[-\frac{(x_{\mathrm{D}} - x'_{\mathrm{D}})^2 + y_{\mathrm{D}}^2}{4\tau}\right]\mathrm{d}\tau \tag{21}$$

$$W\left[\frac{r_{\mathrm{D}}^2(x'_{\mathrm{D}})}{4t_{\mathrm{D}}}, n\pi r_{\mathrm{D}}(x'_{\mathrm{D}})\right] = \int_{r_{\mathrm{D}}^2(x'_{\mathrm{D}})/4t_{\mathrm{D}}}^{\infty} \frac{1}{u}\exp\left[-u - \frac{n^2\pi^2 r_{\mathrm{D}}^2(x'_{\mathrm{D}})}{4u}\right]\mathrm{d}u = \int_0^{t_{\mathrm{D}}} \frac{1}{\tau}\exp\left[-n^2\pi^2\tau - \frac{(x_{\mathrm{D}} - x'_{\mathrm{D}})^2 + y_{\mathrm{D}}^2}{4\tau}\right]\mathrm{d}\tau \tag{22}$$

Substituting Eqs. (21) and (22) and into Eq. (19) results in

$$s_{\mathrm{HD}}(t_{\mathrm{D}}) = \frac{\sqrt{\pi}}{2L_{\mathrm{D}}}\int_0^{t_{\mathrm{D}}} \frac{1}{\sqrt{\tau}}\left(\mathrm{erf}\left[\frac{(L_{\mathrm{D}}/2) + x_{\mathrm{D}}}{2\sqrt{\tau}}\right] + \mathrm{erf}\left[\frac{(L_{\mathrm{D}}/2) - x_{\mathrm{D}}}{2\sqrt{\tau}}\right]\right) \times \exp\left[-\frac{y_{\mathrm{D}}^2}{4\tau}\right] \times \left[1 + 2\sum_{n=1}^{\infty}\cos[n\pi z_{\mathrm{D}}]\cos[n\pi z_{\mathrm{wD}}]\exp[-n^2\pi^2\tau]\right]\mathrm{d}\tau \tag{23}$$

Eq. (23) is the solution for an observation piezometer. The solution for a partially penetrating observation vertical-well with a screen from z_1 to z_2 is

$$\bar{s}_{\mathrm{HD}}(t_{\mathrm{D}}) = \frac{1}{z_{2\mathrm{D}} - z_{1\mathrm{D}}}\int_{z_{1\mathrm{D}}}^{z_{2\mathrm{D}}} s_{\mathrm{HD}}\mathrm{d}z_{\mathrm{D}} \tag{24}$$

where $z_{2D} = z_2/d$ and $z_{1D} = z_1/d$ are the dimensionless z_2 and z_1, respectively.

The solution for a fully penetrating observation vertical-well is

$$\bar{s}_{HD}(t_D) = \int_0^1 s_{HD} dz_D \quad (25)$$

It is interesting to point out that, after changing to the dimensional format, Eq. (23) agrees with what is reported in the petroleum literature, which uses different means to derive the fluid pressure change, such as source function and Green's function methods (Gringarten and Ramey, 1973; Daviau et al., 1988, Table 1; Ozkan et al., 1989, Eq. (1)). The method presented in this study has a potential for application for different well configurations. For instance, by obtaining the point source solution first, we are able to find solutions for vertical, horizontal, inclined, and even curved line sources. Furthermore, the volume integrations of the point source solution may yield solutions for finite-diameter vertical, horizontal, inclined, and curved wells. Further discussion of applying the method for different well configurations is beyond of the scope of this paper and will be reported elsewhere.

2.3. Short and long time approximations of drawdowns in anisotropic confined aquifers

2.3.1. Short time approximation

Drawdown of horizontal-well pumping commonly shows a three-stage profile, i.e. an early, an intermediate, and a late stage (Daviau et al., 1988; Ozkan et al., 1989; Zhan and Cao, 2000). The short time approximation of drawdown has been studied before and is briefly summarized below. The drawdown at the early stage is:

$$s \cong \beta \frac{Q}{4\pi L\sqrt{K_h K_z}} \ln \frac{2.25 t K_h K_z}{S_s[K_z y^2 + K_h(z - z_w)^2]} \quad \text{if } \frac{S_s[K_z y^2 + K_h(z - z_w)]^2}{4tK_h K_z} < 0.01 \quad (26)$$

where $\beta = 1$ if $|x| \leq L/2$; $\beta = 0$ if $|x| > L/2$. The time limits for short time approximation are (Daviau et al., 1988, p. 717):

$$t \leq 0.08(z_w^2 S_s/K_z) \ \text{ if } z_w/d \leq 0.5; \qquad t \leq 0.08(d - z_w)^2 S_s/K_z \ \text{ if } z_w/d > 0.5 \quad (27)$$

and

$$t \leq S_s(L/2 - |x|)^2/(6K_z) \quad (28)$$

The ending time of the intermediate stage is approximately (Daviau et al., 1988, p. 718)

$$0.8S_s(L/2)^2/K_z < t < 3S_s(L/2)^2/K_z \quad (29)$$

It is worthwhile to point out that Eqs. (27)–(29) only give order-of-magnitude estimations; other authors may use slightly different formulae (Murdoch, 1994, p. 3027).

2.3.2. Long time approximation

After the intermediate stage, the equipotential surface in the far field is similar to a cylinder. The drawdown at this late stage is approximated as (Rosa and Carvalho, 1989):

$$s = \frac{Q}{4\pi K_h d}\left[\ln \frac{2.25 K_h t}{S_s(L/2)^2} + \alpha\right] \quad (30)$$

where α is called geometrical skin factor and it is modified from the solution of Rosa and Carvalho (1989, Eqs. (44) and (46)):

$$\begin{aligned} \alpha = {} & 2 \\ & + \frac{1}{2}\left\{\left(\frac{x_D}{L_D/2} - 1\right)\ln\left[\left(\frac{y_D}{L_D/2}\right)^2 + \left(\frac{x_D}{L_D/2} - 1\right)^2\right]\right. \\ & \left. - \left(\frac{x_D}{L_D/2} + 1\right)\ln\left[\left(\frac{y_D}{L_D/2}\right)^2 + \left(\frac{x_D}{L_D/2} + 1\right)^2\right]\right\} \\ & - \frac{y_D}{L_D/2}\left[\tan^{-1}\left(\frac{x_D + L_D/2}{y_D}\right) - \tan^{-1}\left(\frac{x_D - L_D/2}{y_D}\right)\right] \\ & + 2\sum_{n=1}^{\infty} \cos(n\pi z_{wD})\cos(n\pi z_D) \int_{x_D/(L_D/2) - 1}^{x_D/(L_D/2) + 1} \\ & \times K_0\left(n\pi \frac{L_D}{2}\sqrt{u^2 + \left(\frac{y_D}{L_D/2}\right)^2}\right) du \end{aligned} \quad (31)$$

Eq. (31) is the geometrical skin effect for an observation piezometer. The geometrical skin effects for a partially penetrating observation well and a fully penetrating observation well are easily calculated using the similar average schemes of Eqs. (24) and

(25). We have written a program CHOW to numerically calculate the geometrical skin effect of Eq. (31) (Additional information on program CHOW is provided in Section 3.2).

Now we use Eq. (31) to derive the closed-form analytical solution of α at the horizontal-wellbore. As pointed out in previous studies (Daviau et al., 1988; Rosa and Carvalho, 1989), drawdown at an equivalent point of the wellbore ($=0.68$ of the half-well-length from the well center) when using the uniform-flux boundary is very close to the uniform-head boundary solution. Thus we calculate α at $x_D/(L_D/2)=0.68$, $y_D=0$, and $z_D=z_{wD}+r_{wD}$, where r_w is the radius of the horizontal-well and $r_{wD}=r_w/d$. After a few simple calculations, Eq. (31) becomes

$$\alpha = 2-0.6+\frac{2}{\pi L_D}\sum_{n=1}^{\infty}\frac{1}{n}[\cos(n\pi[2z_{wD}+r_{wD})] + \cos(n\pi r_{wD})] \times\left[\int_0^{1.68n\pi L_D}K_0(u)\mathrm{d}u+\int_0^{0.32n\pi L_D}K_0(u)\mathrm{d}u\right] \quad (32)$$

The horizontal-well half-length is usually larger than the aquifer thickness ($L_D>1$) in hydrological applications (Tarshish, 1992; Zhan, 1999). Considering the following identity (Hantush, 1964)

$$\int_0^w K_0(u)\mathrm{d}u=\frac{\pi}{2}\ \text{ if } w\geq\pi \quad (33)$$

Thus

$$\int_0^{1.68n\pi L_D}K_0(u)\mathrm{d}u=\frac{\pi}{2};$$

and

$$\int_0^{0.32n\pi L_D}K_0(u)\mathrm{d}u=\frac{\pi}{2}\ \text{ if } 0.32nL_D\geq 1$$

The condition $0.32nL_D\geq 1$ is satisfied for $n\geq 3$ and $L_D\geq 1.04$. For $n=1$, and 2, this approximation may result in a slightly over-estimated α if L_D is not much larger than 1. In practice, Eq. (32) is approximated as

$$\alpha = 1.4+\frac{2}{L_D}\sum_{n=1}^{\infty}\frac{1}{n}[\cos(n\pi[2z_{wD}+r_{wD}]) + \cos(n\pi r_{wD})] \quad (34)$$

Using the identity

$$\sum_{n=1}^{\infty}\frac{\cos(an)}{n}=\frac{1}{2}\sum_{n=1}^{\infty}\frac{(e^{ia})^n+(e^{-ia})^n}{n} = -\frac{1}{2}\ln[1-e^{ia}]-\frac{1}{2}\ln[1-e^{-ia}] = -\frac{1}{2}\ln[2-2\cos(a)] \quad (35)$$

where $i=\sqrt{-1}$ is the complex sign, and considering the fact that $r_{wD}\ll 1$, then Eq. (34) becomes

$$\alpha = 1.4-\frac{1}{L_D}\ln[4(1-\cos[\pi(2z_{wD}+r_{wD})])(1 - \cos[\pi r_{wD}])] = 1.4-\frac{1}{L_D}\ln[2\pi^2 r_{wD}^2(1-\cos[\pi(2z_{wD}+r_{wD})])] \quad (36)$$

Furthermore, if the horizontal-well is in the middle of the aquifer, $z_{wD}=1/2$, then α becomes

$$\alpha = 1.4-\frac{2}{L_D}\ln[2\pi r_{wD}] = 1.4+\frac{2d}{L}\sqrt{\frac{K_h}{K_z}}\ln\left[\frac{d}{2\pi r_w}\right] \quad (37)$$

We can use Eq. (36) for a general well position or Eq. (37) for a center well to calculate the wellbore geometrical skin effect α.

It is interesting to point out that the above Eq. (36) agrees with Eq. (12) of Hantush and Papadopulos (1962) if choosing a single horizontal-well, i.e. $N=1$ in their Eq. (12). The slight difference is that we evaluate the geometrical skin effect at 0.68 of the half-well-length from the well center, but Hantush and Papadopulos (1962) evaluated the geometrical skin effect at the end of the well, i.e. at $x_D/(L_D/2)=1$. If the geometrical skin effect at the well end is also evaluated, our solution is identical to that of Hantush and Papadopulos (1962). Unfortunately, no detail was given in Hantush and Papadopulos (1962) to show their derivation. We need to point out that the geometrical skin effect at the well end is not suitable for calculating the average wellbore drawdown in our case. The geometrical skin effect at the equivalent point (around 0.68 of the half-well-length) offers the closest approximation of the average geometrical skin effect along the wellbore.

3. Applications on horizontal-well pumping test interpretation in anisotropic confined aquifers

The previous discussion of fluid flow to a horizontal-well will guide us for the horizontal-well pumping test interpretation.

3.1. Semilog analysis of drawdown of a horizontal-well

From the above analysis, it is interesting to find out that the dimensionless drawdowns at the short and long times are proportional to the logarithm of dimensionless time. Thus, plotting drawdown and time in a semilog paper will yield two straight lines for the early and late pumping stages. This is similar to the Cooper and Jacob method used in the vertical-well pumping test interpretation (Cooper and Jacob, 1946). A slight difference is that a geometrical skin factor α is included in the late time approximation in this paper.

We can find $\sqrt{K_h K_z}$ from the slope of the straight line of the early data (Eq. (26)) using $\sqrt{K_h K_z} = 2.3Q/(4\pi L \times \text{slope})$. Extending the straight line to find the intercept point $(0, t_0)$ with axis $s = 0$ yields $S_s = 2.25 K_h K_z t_0/[K_z y^2 + K_h(z - z_w)^2]$. It is clear that, only when both K_h and K_z are known, can S_s be calculated. K_h and K_z can be found when choosing at least two monitoring points.

K_h can also be found from the slope of the straight line of the late data using $K_h = 2.3Q/(4\pi d \times \text{slope})$. Extending the straight line to find the intercept point $(0, t_0)$ with axis $s = 0$ yields $S_s = e^{\alpha} \times 2.25 K_h t_0/(L/2)^2$, where α is the geometrical skin effect calculated from Eq. (31) for a general monitoring point or from Eq. (36) or (37) for a wellbore point. At least two monitoring points are needed to find K_z and S_s. This is done by running the CHOW program with different values of K_z until S_s obtained from two monitoring points agrees with each other.

Several practical aspects should be addressed.

1. In a practical sense, the drawdown data of the early radial flow and the late pseudoradial flow may not always be available in a pumping test. For instance, given $z_w/d = 0.5$, $d = 10$ m, $L = 20$ m, $S_s = 0.005\ \text{m}^{-1}$, and $K = 40$ m/day, the top and bottom boundaries will influence the flow at about $t \approx 0.001$ days, or 1.44 min according to Eq. (27). Therefore, the early radial flow period is too short to be detected. The pseudoradial flow starts at time $14.4 < t < 43.2$ min (see Eq. (29)), indicating that a one-day pumping test will be suitable to generate sufficient measurements for the late pseudoradial flow.
2. Horizontal-wells are often used in extracting fluids (either water or oil) from low-permeability strata owing to their large intercept areas with the formations. If a horizontal-well is in a low-permeability zone and/or the well is long, it may take a very long time to attain the late pseudoradial flow, requiring that we rely on the early radial flow data for the interpretation. As an example, given $z_w/d = 0.5$, $d = 10$ m, $L = 20$ m, $S_s = 0.005\ \text{m}^{-1}$, but $K = 0.1$ m/day, the top and bottom boundaries will affect the flow at $t \approx 0.4$ days $= 9.6$ h (see Eq. (6)), and the late pseudoradial flow starts at $6 < t < 15$ days. Therefore, the early radial flow drawdowns are favorable for the interpretation, as the late pseudoradial flow takes too long to start, indicating that it may not be reached within the limited pumping duration.
3. Mucha and Paulikova (1986) and Moench (1997) pointed out that the hydraulic conductivity and specific storativity could not be accurately evaluated without taking special precautions to eliminate effect of wellbore storage from the early test data. Black and Kipp (1977) and Moench (1997) also pointed out that the delayed observation piezometer response was also important in interpreting the aquifer test. Lissey (1967) and Butler et al. (1996) argued that the delayed piezometer response can be avoided if using a transducer placed below a packer located just above the screen and effectively reduced the standpipe radius to zero. In this paper, these effects (wellbore storage and delayed piezometer response) are not considered.

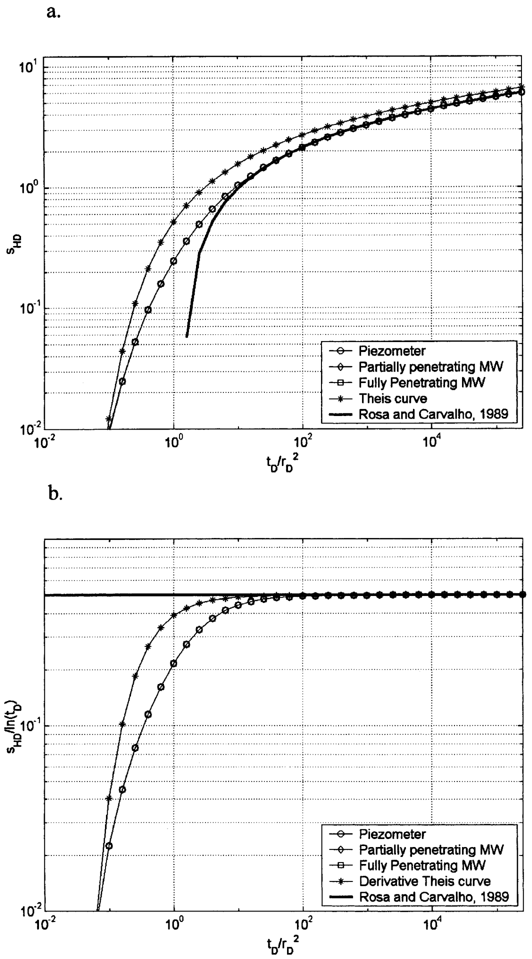

Fig. 2. Comparison of type curves generated using Eq. (23), Theis equation, and Rosa and Carvalho (1989, Eq. (44)) in an isotropic aquifer. The aquifer is 10 m thick. The horizontal-well is 100 m long and at the center of the aquifer. Locations of the monitoring piezometer, the partially and the fully penetrating monitoring wells are at $(x, y, z) = (10\text{ m}, 10\text{ m}, 5\text{ m})$; $(x, y, z_1, z_2) = (10\text{ m}, 10\text{ m}, 4\text{ m}, 6\text{ m})$, and $(x, y) = (10\text{ m}, 10\text{ m})$, respectively. (a) Type curve, (b) Derivative type curve.

3.2. Type curves and derivative type curves of drawdown of horizontal-wells

The disadvantage of the semilog method is that it cannot interpret the intermediate pumping stage. To overcome this, we develop type curves and derivative type curves of horizontal-wells for the entire pumping time. The type curve plots the dimensionless drawdown s_{HD} versus t_D/r_D^2 in a log–log paper, where $r_D^2 = x_D^2 + y_D^2$ is the square of the dimensionless horizontal distance from the observation well to the center of the horizontal-well. The derivative type curve plots the derivative of dimensionless drawdown over the logarithm of the dimensionless time ($ds_{HD}/d(\ln t_D)$) as a function of t_D/r_D^2 in a log–log paper.

The type curve method is commonly used in vertical-well hydraulics (Bear, 1979). The type curve of a fully penetrating vertical-well in a confined aquifer only has one changing parameter t_D/r_D^2, while the type curve of a horizontal-well has six changing parameters t_D, L_D, z_{wD}, x_D, y_D, and z_D (see Eq. (23)).

The derivative type curve method usually improves the diagnostic and quantitative analysis of slug test and pumping test data because it is more sensitive to the small change of drawdown, which would be otherwise less obvious with the standard type curve method (Chow, 1952; Ozkan et al., 1989; Spane and Wurstner, 1993). This method was first proposed by Chow (1952), and was then used in both petroleum engineering (Tiab and Kumar, 1980; Ozkan et al., 1989; Kuchuk et al., 1991; Ahmed and Badry, 1993) and in hydrology (Karasaki et al., 1988; Ostrowski and Kloska, 1989; Spane and Wurstner, 1993).

We have written a program CHOW to generate the type curves and the derivative type curves of horizontal wells on the basis of Eqs. (23)–(25). This program is also used in Section 2.3.2 to calculate the geometrical skin effect. CHOW is published in the first author's website http://geoweb.tamu.edu/Faculty/Zhan/Research.html and can be freely downloaded. Several characteristics of CHOW are discussed below:

1. It is written in a MATLAB® M-file (MathWorks, 2000) with a graphical interface, thus is very easy to use. It uses Gaussian Quadrature method (Press et al., 1989) to calculate the integration of Eq. (23).
2. It can either directly calculate the drawdown at any given observation well at any given time, or generate the dimensionless type curve or the derivative type curve for any observation well to match the real drawdown data. It can handle a fully or a partially penetrating observation well, or an observation piezometer.

Now we discuss the characteristics of type

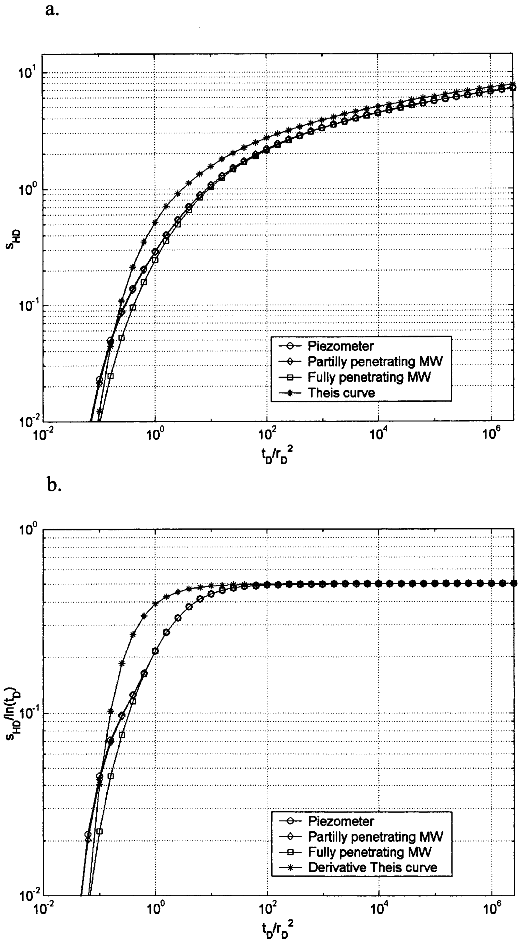

Fig. 3. Comparison of type curves generated using Eq. (23), and Theis equation in an anisotropic aquifer ($K_z/K_h = 0.1$). The aquifer is 10 m thick. The horizontal-well is 100 m long and at the center of the aquifer. Locations of the monitoring piezometer, the partially and the fully penetrating monitoring wells are at $(x, y, z) = (10\ \mathrm{m}, 10\ \mathrm{m}, 5\ \mathrm{m})$; $(x, y, z_1, z_2) = (10\ \mathrm{m}, 10\ \mathrm{m}, 4\ \mathrm{m}, 6\ \mathrm{m})$, and $(x, y) = (10\ \mathrm{m}, 10\ \mathrm{m})$, respectively. (a) Type curve, (b) Derivative type curve.

curves and derivative type curves of horizontal-wells.

Case 1. Type curves and derivative type curves of different monitoring scenarios

This case tests the sensitivity of type curves and derivative type curves on different monitoring scenarios. Fig. 2 shows the type curves and derivative type curves for a piezometer, a partially and a fully penetrating monitoring wells at $x = 10$ m and $y = 10$ m. A piezometer gives a drawdown at a point, a partially penetrating monitoring well gives an averaged drawdown over the screen interval, and a fully penetrating monitoring well gives an averaged drawdown over the aquifer thickness.

The aquifer is 10 m thick and is assumed to be isotropic. The horizontal-well is 100 m long and is at the center of the aquifer ($z_w = 5$ m). The vertical coordinate of the piezometer is at $z = 5$ m, and the vertical interval of the partially penetrating well is between $z = 4$ m and $z = 6$ m. For comparison, Theis curve and derivative Theis curve of a hypothetical vertical-well are also plotted. The late time approximation of drawdown (Rosa and Carvalho, 1989), shown in Eq. (30), is calculated in CHOW and included in Fig. 2.

Fig. 2(a) and (b) show that the type curves and the derivative type curves of a horizontal pumping well for three different monitoring scenarios (piezometer, partially and fully penetrating vertical-wells) are almost identical in an isotropic aquifer at locations not much close to the horizontal well axis ($y \geq d$). Fig. 2(a) and (b) confirm that the solutions derived from Eq. (23) converge to Rosa and Carvalho's (1989) approximation at late time. The early time type curves are different from the Theis curve, reflecting the different nature of flow to a horizontal-well and to a vertical-well at early time (Daviau et al., 1988; Zhan, 1999; Zhan and Cao, 2000). At late time, however, type curves are similar to the Theis curve, reflecting the similar nature of flow to a horizontal-well and to a vertical-well at late time (Daviau et al., 1988; Zhan, 1999; Zhan and Cao, 2000). The slight differences between the type curves of a horizontal-well and the Theis curve are caused by the geometrical skin effects of the horizontal-well (see Eq. (31)).

The differences between the derivative type curves of a horizontal-well and the derivative Theis curve at early time are also obvious in Fig. 2(b). The derivative type curves converge to a constant at late time in Fig. 2(b). This is because s_{HD} is proportional to $\ln(t_D)$ at late time (see Eq. (30)).

Case 2. Type curves and derivative type curves in an anisotropic aquifer

This case tests the sensitivity of type curves and derivative type curves on the aquifer anisotropy. Fig. 3(a) and (b) show the type curves and derivative type curves of a horizontal-well for a piezometer, a

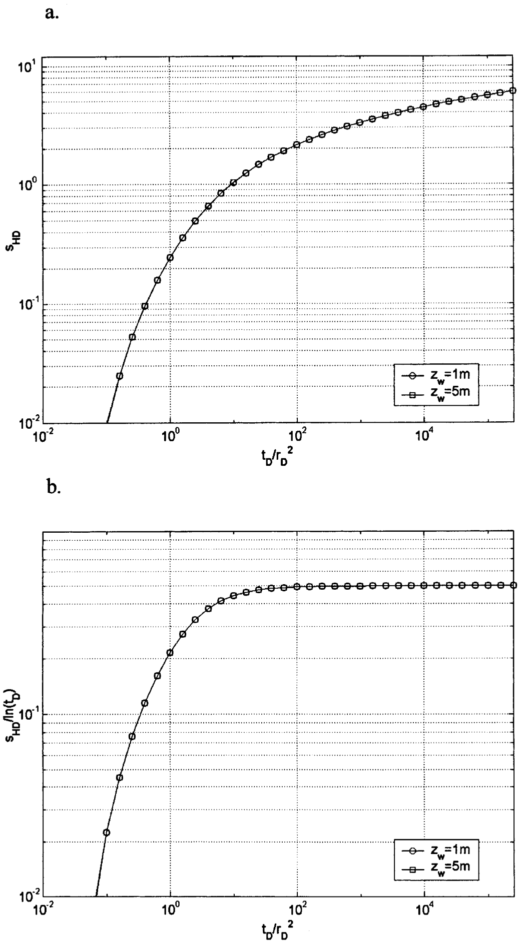

Fig. 4. Comparison of type curves for two pumping well locations in an anisotropic aquifer. The aquifer is 10 m thick. The two wells are 1 and 5 m from the bottom of the aquifer. The well length is 100 m. The monitoring piezometer is at $(x, y, z) = (10\text{ m}, 10\text{ m}, 5\text{ m})$. (a) Type curve, (b) Derivative type curve.

partially and a fully penetrating vertical-wells in an anisotropic aquifer. The setup is identical to that of Case 1 except that the aquifer is anisotropic with $K_z/K_h = 0.1$. Theis curve and derivative Theis curve are also plotted for reference.

Fig. 3(a) and (b) show that the type curves and derivative type curves of three different monitoring scenarios are slightly separated at early time. Those three type curves are almost identical in an isotropic aquifer (Fig. 2(a) and (b)). Fig. 3(a) and (b) indicate that drawdown is somewhat sensitive to the vertical coordinate in an anisotropic aquifer ($K_z < K_h$) at early time when the monitoring point is not far from the horizontal well axis ($y \leq d$). If the monitoring point is far from the horizontal well axis ($y \gg d$), the early time drawdown becomes less sensitive to the vertical coordinate in an anisotropic aquifer ($K_z < K_h$). This result is similar to what has been found for a partially penetrating vertical well (Bear, 1979). In fact, a horizontal well can be visualized as a series of partially penetrating vertical wells, thus it is not surprising to see similarity of the drawdowns near a horizontal well and near a partially penetrating vertical well. The Theis curve, on the other hand, is independent of the anisotropy since it only includes horizontal flow.

Case 3. Type curves and derivative type curves with different horizontal-well locations

This case tests the sensitivity of type curves and derivative type curves on horizontal-well locations. Fig. 4(a) and (b) show the type curves and derivative type curves of a piezometer for two different horizontal-well locations. One is at the center of the aquifer ($z_w = 5$ m) and the other is near the bottom of the aquifer ($z_w = 1$ m). The rest setup is identical to that described in case 1. Fig. 4(a) and (b) show that the type curves and derivative type curves are insensitive to the horizontal pumping well locations for a monitoring point at $(x, y, z) = (10\text{ m}, 10\text{ m}, 5\text{ m})$.

The result revealed in Fig. 4(a) and (b) can be understood by examining the early time drawdown formula (26). That equation shows that when the monitoring well is not much close to the horizontal well ($y \geq d$), the change of z_w has limited influence upon the drawdown. Hydrologically speaking, this indicates that drawdowns at regions not close to the well ($y \geq d$) are primarily controlled by the horizontal flow components. The similar conclusion is found in the study of a partially penetrating vertical well (Bear, 1979). This finding once again confirms the similarity between a horizontal well and a partially penetrating vertical well.

Case 4. Type curves and derivative type curves with different horizontal-well length

This case tests the sensitivity of type curves and derivative type curves on the horizontal-well length. Fig. 5(a) and (b) show the type curves and derivative type curves of a piezometer for three different well lengths: 100, 50, and 25 m. All the rest setup is the same as that in case 1. Fig. 5(a) and (b) indicate that

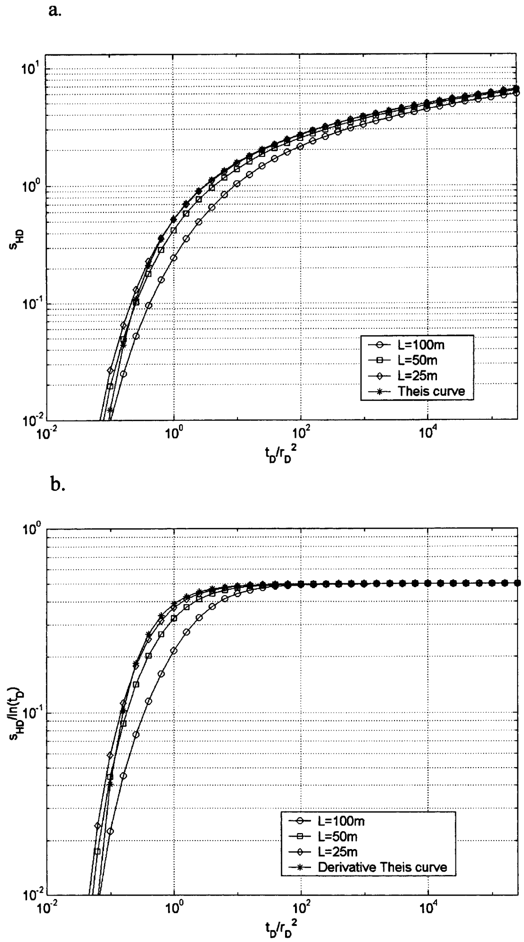

Fig. 5. Comparison of type curves generated using different well lengths and Theis equation in an isotropic aquifer. The aquifer is 10 m thick. The wells are 100, 50, and 25 m long and are at the center of the aquifer. The monitoring piezometer is at $(x, y, z) = (10\text{ m}, 10\text{ m}, 5\text{ m})$. (a) Type curve, (b) Derivative type curve.

the shorter of the horizontal-well, the closer the type curves to Theis curve. Fig. 5(a) and (b) also show that the shorter the well, the faster the type curves converge to the Theis curve. This is easy to understand because a shorter horizontal well is more close to a vertical well. This finding is consistent with previous studies (Daviau et al., 1988; Zhan and Cao, 2000). The same conclusion can be drawn for the derivative type curves.

Fig. 5(a) and (b) also show that the longer the well, the less the dimensionless drawdown at early time. This is because a longer well has less pumping rate per unit screen length (Q/L) that determines the early time drawdown (see Eq. (26)), thus a longer well generates less drawdown at early time.

4. Summary and conclusion

Horizontal-well pumping tests are difficult to interpret because of the influence of aquifer boundaries and well ends. In this paper, a method is proposed to directly solve the boundary problem of flow to a point source in an anisotropic confined aquifer. The point source solution is then used to obtain the drawdown of a horizontal pumping well. The integral formats of drawdowns in Laplace domain and in real time domain are obtained. Analytical approximations of drawdowns at short and long times are discussed. The wellbore geometrical skin effect is analytically derived.

Approximations of drawdowns at short and long times are similar to that of vertical-wells. They are used in the semilog analysis method for horizontal-well pumping test interpretation. The disadvantage is that the semilog method does not use the drawdown data during the intermediate time.

To include the drawdown data during the entire pumping time, a computer program CHOW is written to generate type curves and derivative type curves of horizontal-well pumping. CHOW program numerically calculates Eqs. (23)–(25) using the MATLAB® software. It is graphically integrated and straightforward to use. The program can be freely downloaded from website http://geoweb.tamu.edu/Faculty/Zhan/Research.html.

The CHOW program can generate the type curves and derivative type curves for any of the three kinds of monitoring scenarios: an observation piezometer, a partially penetrating observation well, and a fully penetrating observation well. It can also directly calculate the drawdown for any given observation well at any given time.

The type curves and derivative type curves of a horizontal well depend on well screen length, distance from the well to the lower boundary, aquifer anisotropy, and location of the monitoring well. In general, the type curves and the derivative type curves at early time are different from Theis curve and derivative Theis curve, respectively. This reflects the different nature of flow to a horizontal-well and to a vertical-well at the early time. The type curves converge to

Theis curve except for a geometrical skin effect at late time, reflecting the similar nature of horizontal flow to a horizontal-well and to a vertical-well at late time.

In an isotropic aquifer, the type curves and the derivative type curves at early times are not sensitive to the monitoring scenarios at regions where $y \geq d$. However, they are somewhat sensitive to the monitoring scenarios in an anisotropic aquifer ($K_z < K_h$) at a monitoring point not far away from the horizontal well axis ($y \leq d$). This indicates that the early time drawdown is somewhat sensitive to the vertical coordinate in an anisotropic aquifer ($K_z < K_h$) at a monitoring point not far from the horizontal well axis ($y \leq d$).

The type curves and derivative type curves are insensitive to the horizontal-well location in an isotropic aquifer at a point not much close to the horizontal well axis ($y \leq d$). But they depend on the well lengths. The shorter of the horizontal-well, the closer of the type curve to Theis curve, and the faster the type curve converges to Theis curve. In addition, less drawdown is observed for a longer well at early time for a given total pumping rate. A horizontal well can be visualized as a series of partially penetrating vertical wells and the drawdown near a horizontal well shows similar behavior as the drawdown near a partially penetrating vertical well.

Acknowledgements

Support for this work was provided by the U.S. National Science Foundation Grant No. BES-9909964 and Office of the Vice President for Research and Associate Provost for Graduate Studies, through the Interdisciplinary Research Initiatives Program, Texas A & M University. Thanks to Prof. David Sparks and Mr Steve Desrocher for their review of the manuscript. Thanks to Thomas Engler and two anonymous reviewers for providing suggestions to revise the manuscript.

Appendix A. Appendix

The solution satisfying boundary conditions (13) and (14) can be written (Dougherty and Babu, 1984; Moench, 1997):

$$s'_D(p) = \sum_{n=0}^{\infty} H_n(x_D, y_D, p)\cos(\omega_n z_D) \tag{A1}$$

Substituting Eq. (A1) into Eq. (14) results in

$$\omega_n = n\pi, \quad n = 0, 1, 2, 3, \ldots \tag{A2}$$

Substituting Eq. (A1) into Eq. (12), multiplying bycos($\omega_n z_D$), and integrating from 0 to 1 in the z_D direction will result in

$$\frac{\partial^2 H_0}{\partial x_D^2} + \frac{\partial^2 H_0}{\partial y_D^2} - pH_0 + \frac{2\pi\delta(x_D - x_{0D})\delta(y_D - y_{0D})}{p} = 0 \tag{A3}$$

$$\frac{\partial^2 H_n}{\partial x_D^2} + \frac{\partial^2 H_n}{\partial y_D^2} - (n^2\pi^2 + p)H_n + \frac{4\pi\delta(x_D - x_{0D})\delta(y_D - y_{0D})}{p}\cos(n\pi z_{0D}) = 0 \text{ if } n > 0 \tag{A4}$$

Eqs. (A3) and (A4) are the two-dimensional modified Helmholtz equation (Arfken and Weber, 1995, Table 8.5). Using the Table 8.5 of Arfken and Weber (1995), the solutions to Eqs. (A3) and (A4) and are

$$H_0 = \frac{1}{p} K_0(\sqrt{p}[(x_D - x_{0D})^2 + (y_D - y_{0D})^2]^{1/2}) \tag{A5}$$

$$H_n = \frac{2\cos(n\pi z_{0D})}{p} K_0(\sqrt{n^2\pi^2 + p}[(x_D - x_{0D})^2 + (y_D - y_{0D})^2]^{1/2}), \; n > 0 \tag{A6}$$

Substituting Eqs. (A5) and (A6) into Eq. (A1) results in the solution of s'_D.

References

Ahmed, U., Badry, R.A., 1993. Production logging as an integral part of horizontal well transient-pressure test. SPE Formation Eval., 280–286.

Arfken, G.B., Weber, H.J., 1995. Mathematical Methods for Physicists, 4th. Academic Press, San Diego, USA.

Bear, J., 1979. Hydraulics of Groundwater. McGraw-Hill, New York, USA.

Black, J.H., Kipp Jr., K.L., 1977. Observation well response time and its effect upon aquifer test results. J. Hydrol. 34, 297–306.

Butler Jr., J.J., McElwee, C.D., Liu, W., 1996. Improving the quality of parameter estimates obtained from slug tests. Ground Water 34 (3), 480–490.

Chow, V.T., 1952. On the determination of transmissibility and storage coefficients from pumping test data. Am. Geophys. Un. Trans. 33, 397–404.

Cleveland, T.G., 1994. Recovery performance for vertical and horizontal wells using semianalytical simulation. Ground Water 32 (1), 103–107.

Cooper, H.H., Jacob, C.E., 1946. A generalized graphical method for evaluating formation constants and summarizing well field history. Am. Geophys. Un. Trans. 27, 526–534.

Daviau, F., Mouronval, G., Bourdarot, G., Curutchet, P., 1988. Pressure analysis for horizontal-wells. SPE Formation Eval. 3 (4), 716–724.

Dougherty, D.E., Babu, D.K., 1984. Flow to a partially penetrating well in a double-porosity reservoir. Water Resour. Res. 20 (8), 1116–1122.

Falta, R.W., 1995. Analytical solutions for gas-flow due to gas injection and extraction from horizontal-wells. Ground Water 33 (2), 235–246.

Goode, P.A., Thambynayagam, R.K.M., 1987. Pressure drawdown and buildup analysis of horizontal wells in anisotropic media. SPE Formation Eval. 2 (4), 683–697.

Gringarten, A.C., Ramey Jr., H.J., 1973. The use of source and Green's functions in solving unsteady-flow problems in reservoirs. Soc. Petr. Engng J. 13 (10), 285–296.

Gringarten, A.C., Ramey, H.J., Raghavan, R., 1974. Unsteady-state pressure distributions created by a well with a single infinite-conductivity vertical fracture. Soc. Petr. Engng J., 347–360.

Hantush, M.S., 1964. Hydraulics of wells. In: Chow, V.T. (Ed.). Advances in Hydroscience. Academic Press, New York.

Hantush, M.S., Papadopulos, I.S., 1962. Flow of ground water to collector wells. J. Hydraul. Div., Proc. Am. Soc. Civ. Engrs HY 5, 221–244.

Hunt, B., Massmann, J.W., 2000. Vapor flow to trench in leaky aquifer. J. Environ. Engr 126 (4), 375–380.

Karasaki, K., Long, J.C.S., Witherspoon, P.A., 1988. Analytical models of slug tests. Water Resour. Res. 24 (1), 115–126.

Kuchuk, F.J., Goode, P.A., Wilkinson, D.J., Thambynayagam, R.K.M., 1991. Pressure-transient behavior of horizontal wells with and without gas cap or aquifer. SPE Formation Eval., 86–94.

Langseth, D.E., 1990. Hydraulic performance of horizontal wells. , Proceedings of HMCRI's 11th National Conference, SUPERFUND'90. Hazardous Materials Control Research Institute, Washington, DC pp. 398–408.

Lissey, A., 1967. The use of reducers to increase the sensitivity of piezometers. J. Hydrol. 5, 197–205.

MathWorks, Inc., 2000. MATLAB (software), website: www.mathworks.com. Natick, MA, USA.

Moench, A.F., 1997. Flow to a well of finite diameter in a homogeneous, anisotropic water table aquifer. Water Resour. Res. 33 (6), 1397–1407.

Mucha, I., Paulikova, E., 1986. Pumping test using large-diameter production and observation wells. J. Hydrol. 89, 157–164.

Murdoch, L.C., 1994. Transient analyses of an interceptor trench. Water Resour. Res. 30 (11), 3023–3031.

Ostrowski, L.P., Kloska, M.B., 1989. Use of pressure derivatives in analysis of slug test or DST flow period data. Soc. Petr. Engrs, SPE Pap. , 18595.

Ozkan, E., Raghavan, R., Joshi, S.D., 1989. Horizontal-well pressure analysis. SPE Formation Eval. 4 (4), 567–575.

Press, W.H., Flannery, B.P., Teukolsky, S.A., Vetterling, W.T., 1989. Numerical Recipes, the Art of Scientific Computing (FORTRAN version). Cambridge University Press, New York.

Rosa, A.J., Carvalho, R. de S., 1989. A mathematical model for pressure evaluation in an infinite-conductivity horizontal well. SPE Formation Eval. 4 (4), 559–566.

Rushing, J.A., 1997. A semianalytical model for horizontal well slug testing in confined aquifers. PhD Dissertation, Texas A & M University, College Station, Texas.

Sawyer, C.S., Lieuallen-Dulam, K.K., 1998. Productivity comparison of horizontal and vertical ground water remediation well scenarios. Ground Water 36 (1), 98–103.

Spane Jr., F.A., Wurstner, S.K., 1993. DERIV: A computer program for calculating pressure derivatives for use in hydraulic test analysis. Ground Water 31 (5), 814–822.

Tarshish, M., 1992. Combined mathematical model of flow in an aquifer-horizontal well system. Ground Water 30 (6), 931–935.

Tiab, D., Kumar, A., 1980. Application of the p'_D function to interference analysis. J. Petr. Technol., 1465–1470.

Waterloo Hydrogeologic, Inc., 2000. VISUAL MODFLOW, website: www.flowpath.com. Waterloo, Ont., Canada.

Zhan, H., 1999. Analytical study of capture time to a horizontal well. J. Hydrol. 217, 46–54.

Zhan, H., Cao, J., 2000. Analytical and semi-analytical solutions of horizontal well capture times under no-flow and constant-head boundaries. Adv. Water Resour. 23 (8), 835–848.